Solid Earth Discuss., 5, 737–765, 2013
www.solid-earth-discuss.net/5/737/2013/
doi:10.5194/sed-5-737-2013

Solid Earth
Discussions
Open Access

Strength constraints of shallow crustal strata from analyses of mining induced seismicity

M. Alber[1], **R. Fritschen**[2], **and M. Bischoff**[1,*]

[1]Engineering Geology, Ruhr-University Bochum, Germany
[2]DMT GmbH & Co KG, Essen, Germany
[*]now at: BGR, Hannover, Germany

Received: 26 March 2013 – Accepted: 23 April 2013 – Published: 3 June 2013

Correspondence to: M. Alber (michael.alber@rub.de)

Published by Copernicus Publications on behalf of the European Geosciences Union.

Abstract

Stress redistributions around large underground excavations such as coal mines may lead to failure of the surrounding rock mass. Some of these failure processes were recorded as seismic events. In this paper the different failure processes such as rock mass failure or the reactivation of faults are delineated from the seismic records. These are substantiated by rock mechanical analyses including laboratory strength tests on coal measure rocks obtained from underground drilling. Additionally, shear tests on discontinuities in coal measure rocks (slickensides in shale and rough sandstone joints) were conducted to grasp the possible variation of strength properties of faults. Numerical modeling was employed to evaluate the state of stress at the locations where seismic events did occur.

1 Introduction

The strength of shallow crustal strata (< 3 km depth) is of immediate interest for surface structures as well as for underground civil and mining applications. Recently, alternative energy production such as heat mining by the hot dry rock method or unconventional gas (shale gas, coal bed methane or tight gas) calls for the knowledge of strength constraints for shallow crustal rock masses. There is little direct information from full scale experimental approaches on estimates of rock mass strength. Large scale test to failure involve coal pillars of volume 436 m^3 (Wang et al., 1977) and 0.8 m^3 (van Heerden, 1975), respectively. Iron ore specimen of 1 m^3 were tested e.g. by Jahns (1966). For nuclear waste repository at the Hanfort site Hustrulid (1983) described testing on 8 m^3 Basalt and at the Äspö Pillar Experiment in Sweden appox. 11 m^3 of granite were thermally stressed (Andersson, 2007). However the latter tests were performed on rather intact rock volumes to evaluate spalling problems. For estimating the shear strength of a weak bedding plane in coal measure rocks Baczinsky (2000) reported about two tests involving shear planes of sizes 150 m^2 and 270 m^2.

Typically in situ rock mass strength is scaled from laboratory strength test via some empirical failure criteria (Edelbro, 2003). The strength of natural faults is often approximated with Byerlee's law (Byerlee, 1978) which assumes a friction angle φ of 40° for normal stresses on planes $\sigma_N < 200$ MPa and φ of 30° for $\sigma_N > 200$ MPa, respectively. However, for shallow strata down to a depth of 5 km the maximum normal stresses σ_N typically are below 150 MPa. In this range of normal stresses the data of Byerlee (cf. Byerlee, 1978, Figs. 3 and 4) vary considerably.

Mining operations reach nowadays depths of app. 3 km. In the case of coal mines the typically flat or slightly inclined tabular resources are mined out by the longwall method. With this method severe stress redistributions follow the resource extraction as schematically shown in Fig. 1 (Whittaker, 1974). The abutment stresses may lead to the failure of rock mass around the longwall face and/or cause slip of existing faults. Either failure or slip leads to mining-induced seismic events. If a seismic network exists then the processing of seismic events (i.e. location of events and focal analyses) allow rock mechanical investigations with the goal of constraining the failure processes and the strength of the rock mass or faults, respectively. For this purpose seismic events of local magnitude $M_L > 0.6$ were analyzed. The associated area of failure is in the order of 20 m^2 or larger. In the course of the collaborative resource center CRC 526 "Rheology of the Earth" the mining induced seismic events from two coal mines were analyzed with the goal of indentifying failure mechanisms, the stresses leading to those failures and to finally estimate the strength constraints.

2 Locations and geology of the mines

Mine A is located in the German Ruhr mining district. There are some special features about the coal mining operations in the Ruhr area which may be summarized as follows: the depth of mining is currently around 1100 m and the in situ stresses at depth are in the order of 30–40 MPa. The coal measure rocks in the Ruhr mining district are very strong. The strata are jointed, faulted and folded. The faults are

systematically oriented with respect to the variscan folding axes. There exist many old workings in close proximity to the current ones, leading to significant stress concentrations at gob/solid boundaries. Figure 2 shows an aerial view of the longwalls under consideration along with locations of the seismic stations and the orientation of the horizontal stresses. Details on the seismic stations at Mine A are given by Alber et al. (2009).

Mine B is located in the German Saar mining district. The SW–NE striking Saar-Nahe-Basin in SW-Germany is one of the largest permo-carboniferous basins in the internal zone of the Variscides. The structural style within the basin is characterized by normal faults parallel to the basin axis and orthogonal transfer fault zones. At the mine scale the strata are dipping gently to N/NE with some 15°. The longwalls are in virgin rock mass with no previous mining operations as shown in Fig. 3. Details on the seismic stations at Mine B are given by Fritschen (2010).

The strata comprise similar rock types as in Mine A, i.e. mainly sandstone and siltstone, but are slightly weaker. The basic geological and geotechnical data is summarized in Table 1.

3 Mining induced seismic events

3.1 Mining induced seismic events while developing the tunnels

In both mines seismic events were record while driving the tunnels of dimensions 5 m × 5 m surrounding the future longwall operations. The events were assumed at coal seam level and minor damage to the walls of the tunnels was visible. Figure 4a show the locations and the temporal evolution of events in Mine A.

Both, strength failure of the rock mass or fault reactivation could have been the reason for the events. The local seismological network in Mine A allowed for fault plane solutions (Fig. 4b). The assumed fault planes strike N–S or NE–SW with common dips of approximate 60° towards W and are in accordance with the local tectonic features.

The strength of the coal and coal measure rock mass in this stress situation is given in Fig. 5.

Evidently, even the weakest coal measure strata are strong enough and are unlikely to fail. Normal and shear stresses on planes oriented as suggested from focal analyses were calculated for the locations of the seismic events (cf. Fig. 4b). Figure 6 shows those stresses and the required frictional strength (mob φ) for the fault to remain stable. The respective friction angles of mob $\varphi = 18^\circ$ and 8° are quite low.

The seismic network in Mine B was not yet fully developed so that no focal analyses were possible. In Fig. 7 the major and minor principal stresses at depth are given. The typical rock mass strength around the seam at Mine B is well above the stresses and no failure of the rock mass is anticipated. In order to produce failure in the vicinity of the tunnel a suitably oriented fault of with a frictional strength of not more than $\varphi = 20^\circ$ is necessary. The insert the Figure shows the orientation of the stresses and the most probable alignment of the fault planes (dotted lines), which are similar to tectonic features at the mine (cf. Fig. 3).

3.2 Mining induced seismic events during longwall operations

In Mine A more than 6000 events were recorded during longwall operations (Bischoff et al., 2010). The detailed rock mechanical analysis was presented earlier (Alber et al., 2009). For the focus of this paper the situation of underminig a remnant pillar is used for estimating the strength of rock mass or faults. The situation is shown in Fig. 8 where the location of the seismic events as well as the outline of the pillar (approx. 60 m above the coal seam) is also given. By mining the coal seam from SW the induced stresses exceeded the strength of either the rock mass or a fault.

Figure 9 depicts the results of 3-D numerical modeling of the stresses. Here the major and minor principal stresses σ_1 and σ_3, the strength of the rock mass (estimated by the Hoek–Brown parameter UCS = 128, mb = 0.88; s = 0.0055) and the mobilized friction φ (mob $\varphi = \tan^{-1}\tau/\sigma_N$) along a plane parallel to the pillar's W-side. The results suggest that rock mass failure took place in this situation as the major principal

stresses are significantly higher than the rock mass strength σ_{1s} and the minor principal stresses are mainly tensile when approaching the pillar. The activated frictional strength on a fault plane would be in the order of $\varphi = 20$–25°.

While extracting longwall II (cf. Fig. 2) seismic events were recorded close to where events have been localized from advancing the tunnel (Fig. 10 left). Focal analyses suggest normal faulting on both, NW–SE and NW–SW oriented planes. Figure 10 (right) shows the peak particle velocities (PPV) of the events. Again numerical modeling was employed to evaluate the normal and shear stresses on planes oriented as indicated from focal analyses.

These planes are in broad accordance with the strike of local tectonic features. The seismic events took place well ahead of the face, up to approximately 50 to 100 m in front of the actual position of the longwall. Moreover, they were localized at the same place were events were assumed when driving the tunnels two years earlier. Numerical modeling was employed to evaluate the strength of those distinct planes. Stresses were evaluated over a distance of 400 m along a N–S trending line at across the tunnel as shown in Fig. 10b. Figure 11 shows the normalized slip tendency NST = $\tau \tan\varphi/\sigma_N$. Following the approach of Lisle and Srivasta (2004) τ and σ_N are the shear and the normal stress on the respective plane orientation, which are here normalized to a generic friction angle $\varphi = 30^\circ$ This normalized slip tendency ranges always between 0–1 and allow for easy comparison of stressed planes. Figure 11a–d shows in the inserts the respective orientations of the planes. For both lines of strike (NW–SE and NE–SW, respectively) two dip directions were assumed. The differently colored lines depict the distance of the longwall to the line of evaluation as shown in Fig. 10b. Numerical analyses were carried out at 5 positions (330 m, 241 m, 88 m, 32 m) east of the reference point and at a westerly position (−23 m) of the longwall when it passed through.

For the NE–SW oriented planes the SE dipping structures (Fig. 11b) show higher slip tendencies than the NW oriented structures. The highest demand on frictional strength would occur when the longwall is approximately 88 m away (green line). For slip to occur the friction angle should be in the order of 13°.

For the NW–SE oriented planes the SW dipping structures show higher slip tendencies compared to the NE dipping ones. The majority of the NW–SE striking faults in the area of Mine A have exactly this dip direction. When the longwall is 32 m away the normalized slip tendency is in the order of 0.5 to 0.6 which translates to a mobilized friction angle of 16 to 19°.

In Mine B a series of severe mining induced events up to magnitude M_L = 4.0 occurred while excavation a double longwall. By creating a huge underground excavation of 700 m width stresses were induced leading to the slip of faults some 300 above the coal seam (Alber and Fritschen, 2011). Figure 12 shows the normalized slip tendency on a plane 150°/80° (dipdirection/dip) 300 m above the longwalls.

The M_L = 4.0 event was localized at an area where the normalized slip tendency was computed to be 0.6 which translates to a frictional strength of $\varphi = 18°$. It is noteworthy that this 4.0 event took not place at the location of the highest slip tendency.

4 Constraints for the strength of the uppermost crust

The case studies involving mining induced seismic events demonstrate that the strength of the uppermost crust depends to a high degree on the frictional properties of faults. Rock mass failure does often occur when tensile stresses are involved. It was found from back-calculation that the frictional strength of the faults is in the order of 16–20°, in one case as low as 8°. In the evaluated cases water pressure did not play a role in fault strength as it was never encountered during mining. Even if present the underground excavations would act like a sink and drain the rock mass.

Shear tests on discontinuities in coal measure rock on the laboratory scale have been conducted on slickensides in shale and saw-cut sandstones. Friction angles range from 25° for the saw-cut sandstone to 19° for the slickenside in shale as shown in Fig. 13. It may be assumed that for in-situ conditions the friction angles are even lower as for higher normal stresses the slope of the normal /shear stress curve gets typically smaller. This nonlinearity of shear strength is well established in rock mechanics

(Patton, 1966; Barton, 1976). Moreover, when extrapolating shear strength from laboratory test to the size of fault area the roughness as well as the strength of the fault wall rock is thought to decrease (Bandis, 1990).

The sub-variscan rock mass in the area of Mine B has a typical fault pattern with its dominating NW–SE striking normal faults (Fig. 14). The general state of stress is estimated from hydraulic fracturing stress measurements and visualized in Fig. 15.

For any depth $z > 950$ m σ_H is σ_1 and σ_h is σ_3 leading to strike-slip faulting on favorably oriented planes. Sibson (1985) proposed a procedure to estimate the angle θ between σ_H and a fault plane for slip as a function of the static friction angle φ (Fig. 16). For a depth of 1500 m and the lower limit $\varphi = 15°$, as indicated from numerical modeling above, any fault plane within $17° < \theta < 48°$ will slip. Any change of the state of stress towards increasing σ_H or decreasing σ_h will lead to slip on the fault.

5 Discussion

Our results show that faults may be reactivated by very small stress disturbances. Small changes of the ratio σ_1/σ_3 might trigger slip on already critically stresses planes (cf. Fig. 16). However, as pointed out by Fritschen (2010), not all induced events in German coal mines can be attributed to movements on preexisting faults. In the Ruhr area, most recorded seismic events are directly connected with the advancing working faces and show no evident connection to geological faults. Following Gibowicz and Kijko (1994), these two broad types of induced seismic events are observed almost universally, i.e. seismic events directly connected with mining operations, that is, associated with the formation of fractures at stope faces, and seismic events associated with movement on major geologic discontinuities. Whether a fault of low frictional strength exists in the vicinity of an active working panel can be detected by analyzing seismic event locations in relation to the working panel positions. If such a fault exists, then seismicity in greater distance to the working panel or seismicity induced by the driving of tunnels should be observed. The often observed absence of seismicity in greater distance to working

panels suggests that not the whole uppermost crust but only a part of it is controlled by the frictional strength of faults. The strength of these parts, however, cannot be estimated by the frictional properties of faults given by Byerlee (1978).

The frictional properties of fault as given by Byerlee (1978) are considered being too high as Byerlee used triaxial tests on fresh planes of failure for estimating their friction angles. In the cases discussed here the concern is the friction of mature faults. From the point of mining activities it is evident that resource extraction is closely related to, or more pronounced, the cause for seismic events. Al-Saigh and Kuznir (1987) reported about 812 "tremors" over a monitoring period of two years while longwall mining was conducted at a depth of 900 m below surface. The alignment of the longwall close and parallel to a fault was assumed to reactivate the fault. Donelly (2009) reviewed numerous cases of fault activation caused by mining. Some important conclusions drawn by Donelly (2009) are that faults are capable of several phases of reactivation and that delayed activity in faults upon mining is rare. With the situation in Mine A the fault under consideration has probably been activated by the previous 6 longwalls excavated above. The notion that movement of the fault is immediate upon disturbance of the state of stress by mining supports the approach that induced stresses may be resolved on the plane under consideration and being used for estimating their frictional strength.

The back-calculated friction angles of the faults are in the order of 16–20°, in one case as low as 8°. This is not too far of the estimates by Carena and Moder (2009) who estimated from numerical modeling that most crustal faults in California are weak with a friction angle of $\varphi \leq 12°$. The application of the slip tendency method was successfully used for estimating seismic events from stimulation tests at the Groß-Schönebeck geothermal project (Moek et al., 2009). It may be concluded that e.g. for the area around Mine B the faults down to a depth of approximately 1500 m are critically stressed. The seismic event while driving the tunnels during mine development was documented by a small displacement of the tunnel walls in horizontal direction perpendicular to the direction of tunneling. Accordingly strike-slip faulting may be assumed, which is in agreement with the state of stress at a depth of 1400 m (cf. Fig. 16).

The strong seismic events while mining the double longwall occur at a depth of approximately 1100 m and were classified as normal faults from focal analyses. The stress regime at that depth ($\sigma_H \approx \sigma_V > \sigma_h$) as shown in Fig. 16 do not necessarily disagree with the assumed normal faulting as stress rotations (Diederichs et al., 2004) take place around the underground excavations.

In conclusion, the strength constraints of shallow crustal strata as derived from the analyses of mining induced seismicity are mainly dominated by weak faults which are unfavorably oriented to the local stress conditions. The frictional strength of the faults under consideration are in the range of $8° < \varphi < 20°$. Rock mass failure is not likely to happen under typical in-situ stresses but possible under mining induced stress changes.

Acknowledgements. This research was supported by the collaborative research centre "Rheology of the Earth, SFB 526" funded by the German Research Society (DFG). The joint work of rock engineers, mining engineers and geophysicists allowed for the conclusions reached in this research.

References

Alber, M. and Fritschen, R.: Rock mechanical analysis of a M_L = 4.0 seismic event induced by mining in the Saar District, Germany, Geophys. J. Int., 186, 359–372, 2011.

Alber, M., Fritschen, R., Bischoff, M., and Meier, T.: Rock mechanical investigations of seismic events in a deep longwall coal mine, Int. J. Rock Mech. Min., 46, 408–420, 2009.

Al-Saigh, N. H. and Kuznir, N. J.: Some observations on the influence of faults in mining-induced seismicity, Eng. Geol., 23, 277–289, 1987.

Anderson, E. M.: The Dynamics of Faulting, Oliver and Boyd, Edinburgh, 1951.

Andersson, J. C.: Äspö Pillar Stability Experiment – Final Report: Rock Mass Response to Coupled Mechanical Thermal Loading, Technical Report TR-07-01, SKB, Stockholm, 2007.

Baczynski, N. R. P.: Large scale in-situ shear tests for slope design, in: Proc. GeoEng 2000, paper SNEJ0214, 2000.

Bandis, S. C.: Mechanical properties of rock joints, in: Proc. ISRM Symposium on Rock Joints, edited by: Barton, N. and Stephansson, O., 125–140, 1990.
Barton, N. R.: The shear strength of rock and rock joints, Int. J. Rock Mech. Min., 13, 1–24, 1976.
Bischoff, M., Cete, A., Fritschen, R., and Meier, T.: Coal mining induced seismicity in the Ruhr Area, Germany, Pure Appl. Geophys., 167, 63–75, 2010.
Byerlee, J. D.: Friction of rocks, Pure Appl. Geophys., 116, 615–626, 1978.
Carena, S. and Moder, C.: The strength of faults in the crust in the western United States, Earth Planet. Sc. Lett., 287, 373–384, 2009.
Diederichs, M. S., Kaiser, P. K., and Eberhardt, E.: Damage initiation and propagation in hard rock tunnelling and the influence of near-face stress rotation, Int. J. Rock Mech. Min., 41, 785–812, 2004.
Donelly, L. J.: A review of international cases of fault reactivation during mining subsidence and fluid abstraction, Q. J. Eng. Geol. Hydroge., 42, 73–94, 2009.
Durrheim, R. J., Haile, A., Roberts, M. K. C., Schweitzer, J. K., Spottiswoode, S. M., and Klokow, J. W.: Violent failure of a remnant in a deep South African gold mine, Tectonophysics, 289, 105–116, 1998
Edelebro, C.: Rock Mass Strength – a Review, Technical Report 2003:16, Luela University of Technology, Sweden, 2003.
Fossen, H.: Structural Geology, Cambridge University Press, Cambridge, 2010.
Fritschen, R.: Mining-induced seismicity in the Saarland, Germany, Pure Appl. Geophy., 167, 67–89, 2010.
Gibowicz, S. J. and Kijko, A.: An Introduction to Mining Seismology, Academic Press, 1994.
Hustrulid, W. A.: Design of geomechanical experiments for radioactive waste repository, in: Proceedings of the 1st International Symposium of Field Measurements in Geomechanics, edited by: Kovari, K., 1381–1408, 1983.
Jahns, H.: Measuring the Strength of Rock at an Increasing Scale, in: Proceedings of the 1st International Congress of Rock Mechanics, 477–482, 1966.
Lisle, R. J. and Srivastava, D. C.: Test of the frictional reactivation theory for faults and validity of fault-slip analysis, Geology, 32, 569–572, 2004.
Moeck, I., Kwiatek, G., and Zimmermann, G.: Slip tendency analysis, fault reactivation potential and induced seismicity in a deep geothermal reservoir, J. Struct. Geol., 31, 1174–1182, 2009.

Ortlepp, W. D.: Observation of mining-induced faults in an intact rock mass at depth, Int. J. Rock Mech. Min., 37, 423–436, 2000.
Patton, F. D.: Multiple modes of shear failure in rock, in: Proceedings of the 1st Congress of ISRM, 509–513, 1966.
Rummel, F.: Crustal stress derived from fluid injection tests in boreholes, in: In-Situ Characterisation of Rocks, edited by: Sharma, V. M. and Saxena, K. R., 205–244, 2002.
Sibson, R. H.: A note on fault activation, J. Struct. Geol., 7, 751–754, 1985.
Stollhofen, H.: Facies architecture variations and seismogenic structures in the Carboniferous-Permian Saar-Nahe Basin (SW Germany): evidence for extension-related transfer fault activity, Sediment. Geol., 119, 47–83, 1998.
van Heerden, W. L.: In-situ determination of complete stress-strain characteristics of large coal specimen, J. South Afr. Inst. Min. Metall., 75, 207–217, 1975.
Wang, F. G., Skelly, W. A., and Wolgamott, J.: In-situ coal pillar strength study, in: Proceedings of the 18th US Symposium on Rock Mechanics, 2B5-1:9, 1977.
Whittaker, B. N.: A review of progress with longwall mine design and layout, in: Proceedings of the State of the Art of Ground Control in Longwall Mines and Mine Subsidence, AIME, 77–84, 1982.

Table 1. Geological and geotechnical situation at the mines.

Feature	Mine A	Mine B
Depth of longwalls below surface	1100 m	1400 m
$\sigma_V/\sigma_H/\sigma_h$	29/39/18 MPa	34/43/21 MPa
Orientation of σ_H	NW–SE, perpendicular to long axis of longwalls	
Orientation of faults	NNW–SSE/NE–SW	NW–SE/NE–SW
Known faults in area of longwall	Yes (3 or more)	No (1 assumed)
Longwall dimension (W × L)	350 m × 1200 m	700 m × 2000 m (double longwall)
Previous mining	Yes, multiple seam mining	No
Rock mass quality RMR	50–90	60–80
Intact rock strength	Siltstone: (20) 100 MPa Sandstone: 120 MPa	Siltstone: 30–40 MPa Sandstone: 60–80 MPa
Seismic stations	15 surface + 6 subsurface	23 surface + 3 subsurface

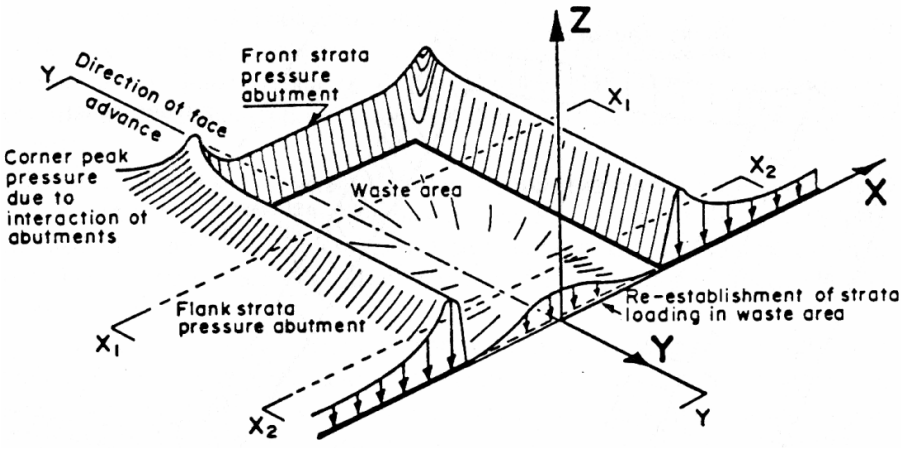

Fig. 1. Abutment stresses around a longwall (Whittaker, 1980).

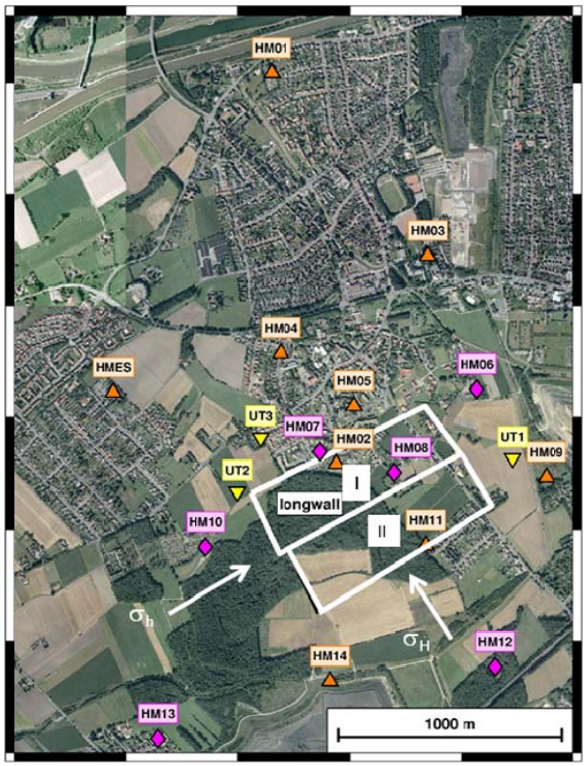

Fig. 2. Aerial view of longwalls, orientation of horizontal stresses and stations (Mine A).

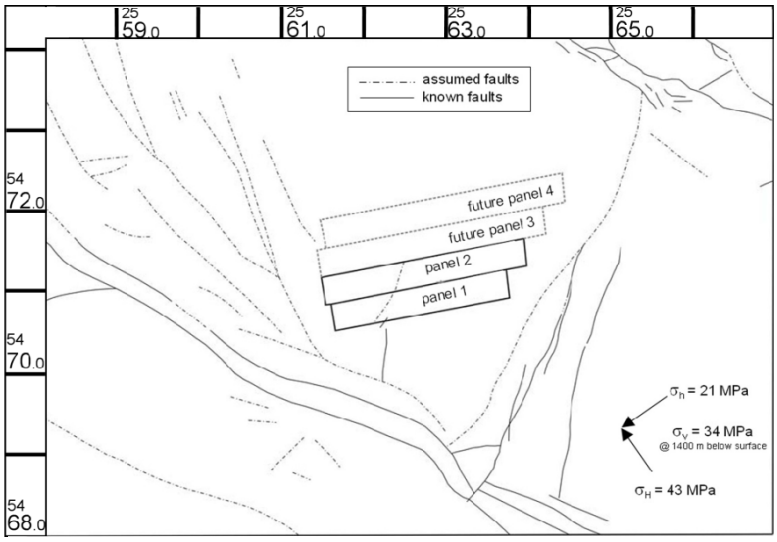

Fig. 3. Plan view of the coal field with faults, double panel 1 and 2 and in-situ stresses at depth (Mine B).

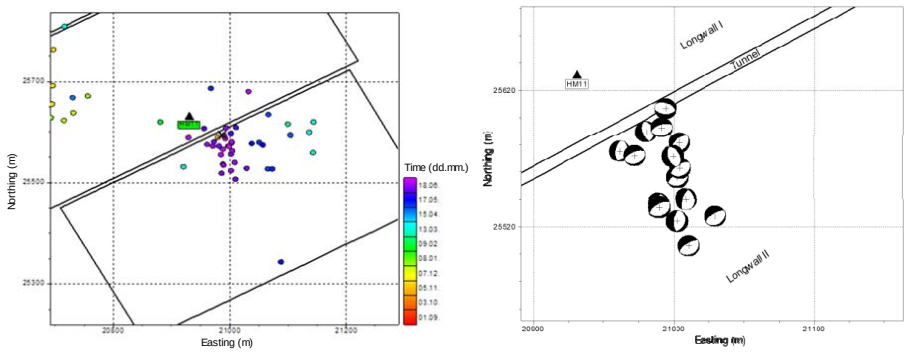

Fig. 4. (left panel) Locations and temporal evalution of the seimic events while tunneling and (right panel) focal analyses of selected seimic events.

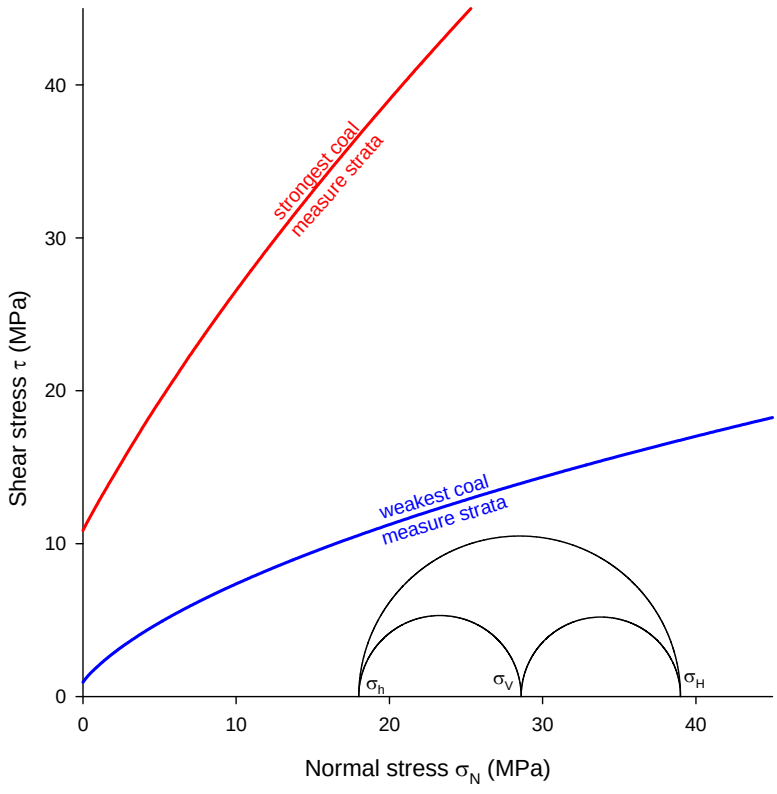

Fig. 5. Mohr circles of the in situ state of stress and strength envelopes of the weakest and strongest rock mass, respectively.

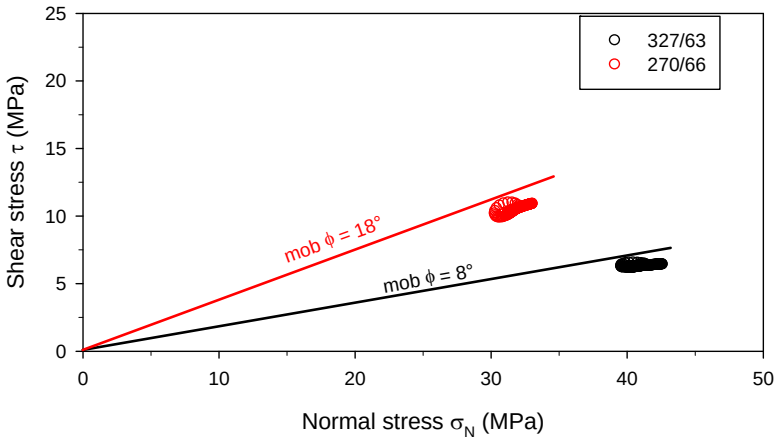

Fig. 6. Numerically evaluated shear and normal stresses on assumed fault planes from focal analyses (cf. Fig. 4b) and associated frictional strength of the planes.

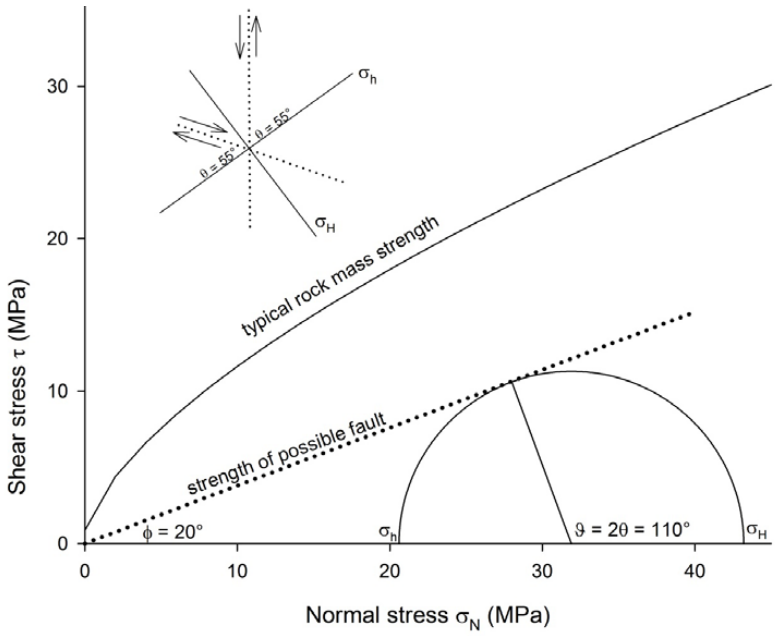

Fig. 7. In-situ stresses at depth and typical rock mass strength at Mine B. The insert shows the preferred fault reactivation orientations (dotted lines) which coincide with the local tectonic features.

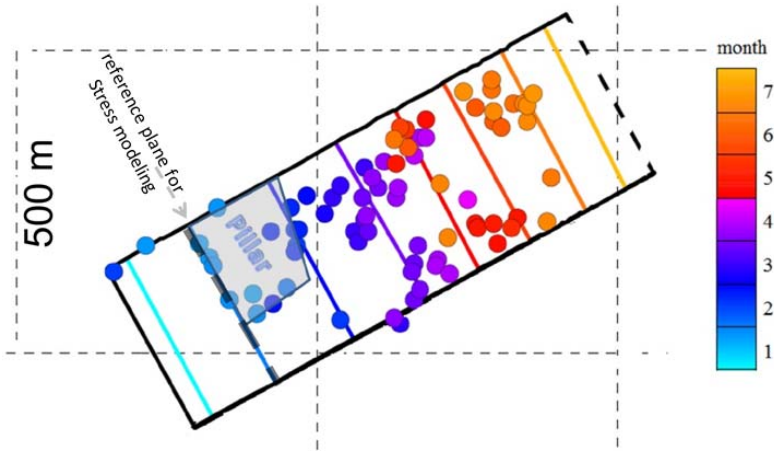

Fig. 8. Location and temporal evolution of seismic events in mime A, longwall I. The coloured lines denote the position of the longwall face by month. Stresses while undermining the remnant pillar 60 m above the longwall were evaluated by numerical modelling.

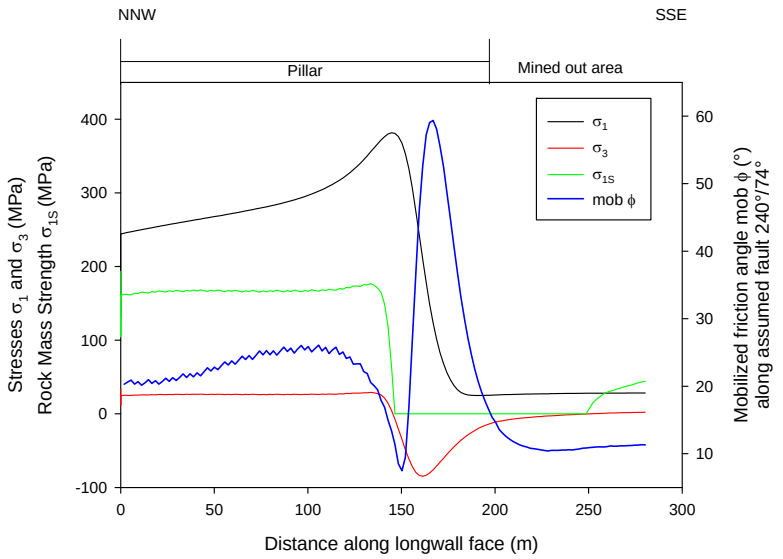

Fig. 9. Principal stresses, rock mass strength and mobilized friction at the level of the undermined remnant pillar.

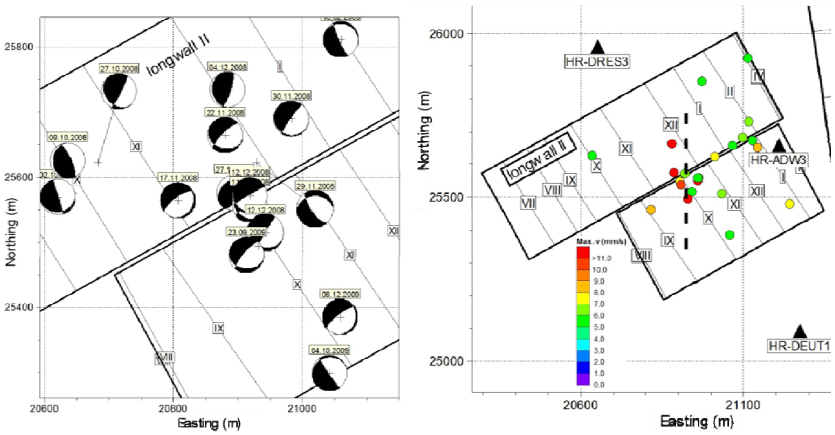

Fig. 10. (left panel) Location and focal analyses of the seismic events while excavating longwall II at Mine B. (right panel) Location and maximum peak particle velocites of the strengest seismic events. Numerical analyses were executed for the various focal planes along the dashed line. The lines with the roman numbers denote the position of the longwall face at the end of the respective month.

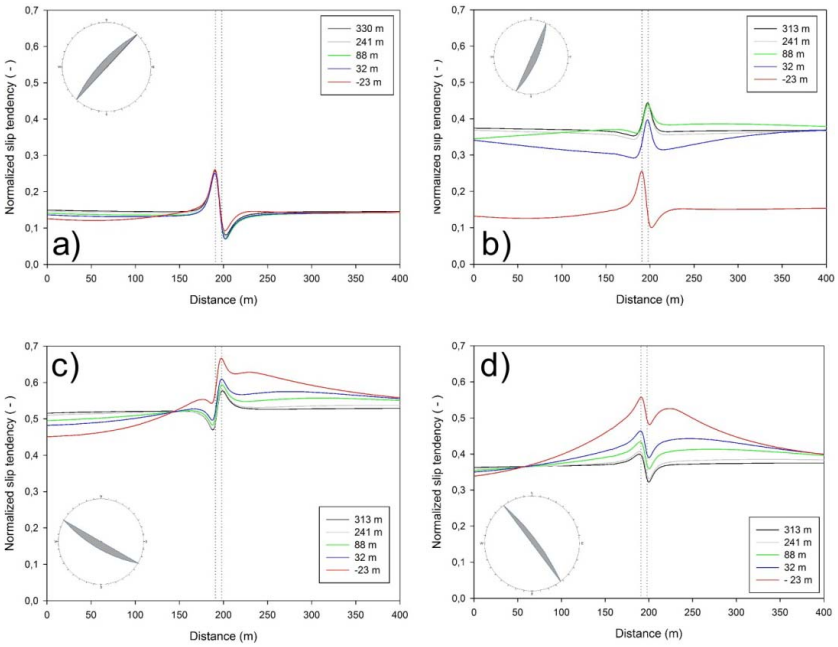

Fig. 11. Normalized slip tendencies along a 400 m long N–S line. The tunnel is at the center. Slip tendencies were calculated for different distances of the longwall to the evaluation line. (**a** and **b**) represent the NE–SW striking planes and (**c** and **d**) represent the NW–SE oriented planes.

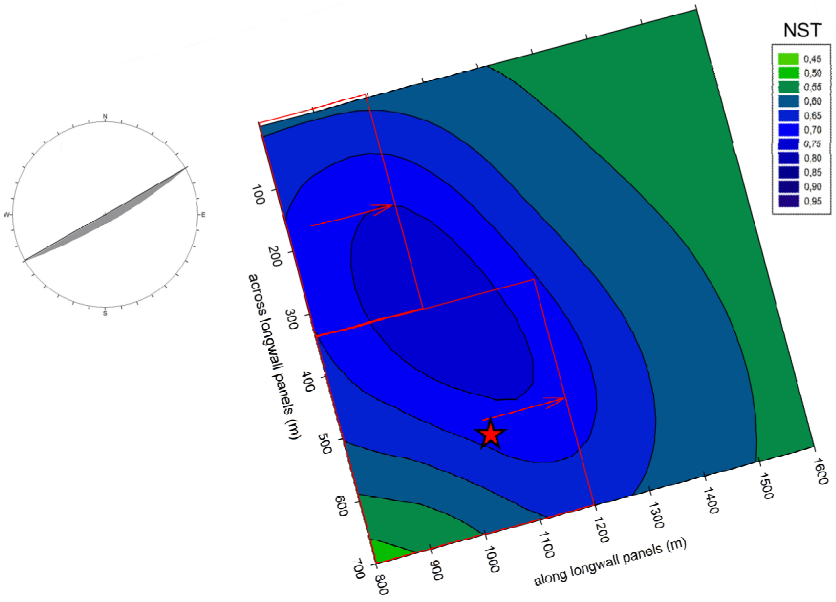

Fig. 12. Normalized slip tendency (NST) of a steep dipping ENE–WSW oriented plane 300 m above the double longwall (red boxes). The red star indicates the location of the M_L = 4.0 event.

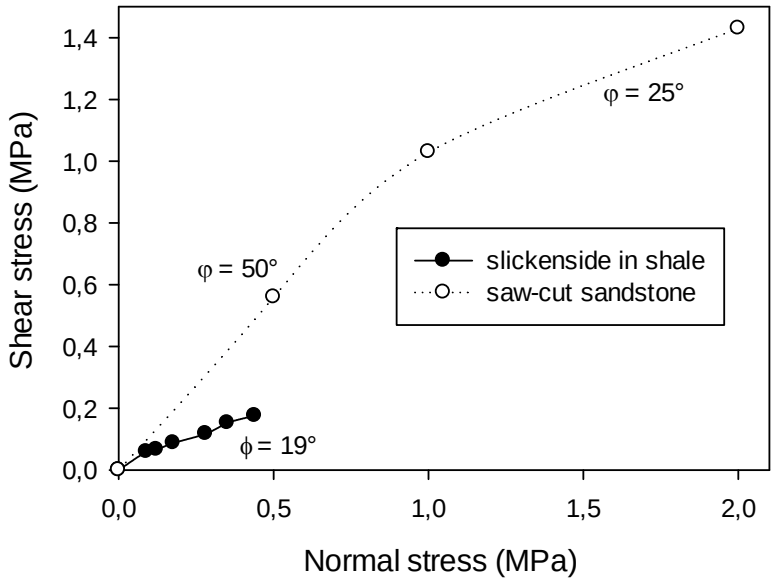

Fig. 13. Frictional strength from laboratory tests on slickensides in shale and saw-cut sandstones from Mine B.

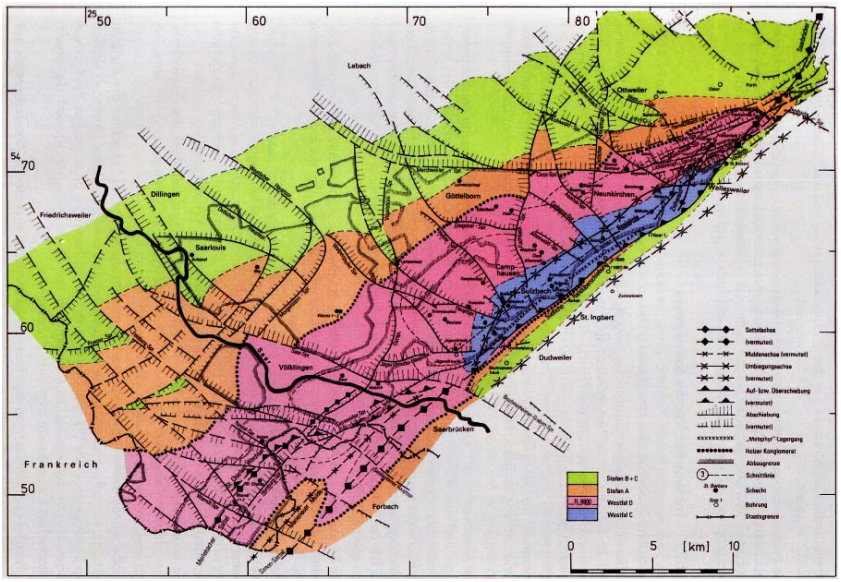

Fig. 14. Geological map of the Saar basin with major faults (modified from Stollhofen, 1998).

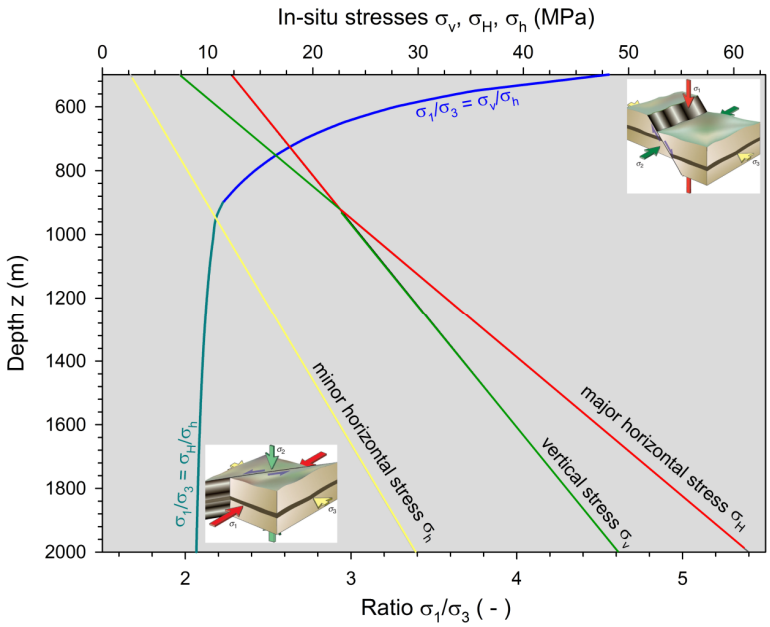

Fig. 15. State of in-situ stresses at Mine B from hydraulic fracturing stress measurements. The major principal stress σ_1 (red line) is at depth to 950 m σ_V, then changes to σ_H. The green line indicates the intermediate principal stress σ_2 (for depth 950 m an deeper) and the yellow line the minor principal stress $\sigma_3 = \sigma_h$ for all depths. The inserts (modified from Fossen, 2010) show the possible fault mechanisms, i.e. normal faulting at shallow depth and strike slip at depth.

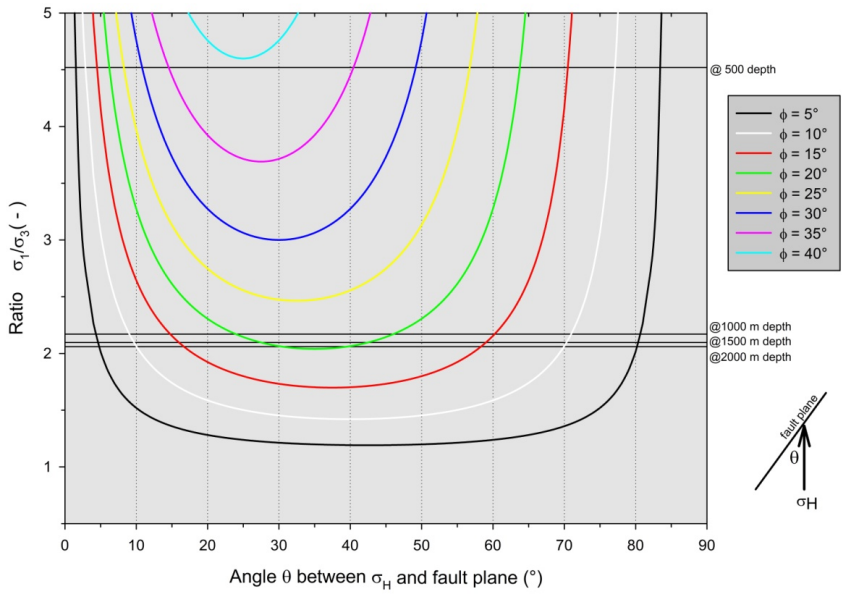

Fig. 16. Application of Sibson's (1985) approach to estimate the angle θ between the major horizontal stress, here σ_H, and a fault plane. Shown are isolines for different friction angles φ of faults in conjunction with the stress ratio σ_1/σ_3 as described in Fig. 15. At depths between 500 and 1000 m faults may fail with friction angle $\varphi < 40^\circ$ when suitably oriented. For depth $z > 1000$ m faults may only slip if their friction angel $\varphi < 20^\circ$ and suitably oriented. For example, a fault with $\varphi = 15^\circ$ may fail at Mine B only if the angle between σ_H and the fault plane is $15^\circ < \theta < 60^\circ$.